Multi-Dimensional Diffusion MRI Sampling Scheme: B-tensor Design and Accurate Signal Reconstruction

Alice Bates, Alessandro Daducci, Emmanuel Caruyer

Multi-Dimensional Diffusion MRI Sampling Scheme: B-tensor Design and Accurate Signal Reconstruction

Alice Bates[1], Alessandro Daducci[2], and Emmanuel Caruyer[3]

[1]Research School of Engineering, Australian National University, Canberra, Australia, [2]Computer Science department, University of Verona, Verona, Italy, [3]Univ Rennes, Inria, CNRS, IRISA, Rennes, France

Synopsis

b-tensor encoding enables the separation of isotropic and anisotropic tensors. However, little consideration has been given as to how to design a b-tensor encoding sampling scheme. In this work, we propose the first 4D basis for representing the diffusion signal acquired with b-tensor encoding. We study the properties of the diffusion signal in this basis to give recommendations for optimally sampling the space of axisymmetric b-tensors. We show, using simulations, that the proposed sampling scheme enables accurate reconstruction of the diffusion signal by expansion in this basis using a clinically feasible number of samples.

Introduction

Multi-dimensional diffusion MRI (MD-dMRI) is a recent diffusion signal modelling and reconstruction framework where the diffusion signal is derived from the diffusion tensor distribution (DTD). Advanced magnetic gradient modulation schemes, resulting in b-tensor encoding, enable separation of isotropic and anisotropic tensors[1-3]. Often diffusion tensors are assumed to be axisymmetric, so the DTD is 4D[4,5]. While algorithms have been proposed for recovering the DTD from b-tensor encoded measurements of the diffusion signal[4-6], little consideration has been given to the b-tensor sampling scheme. Currently, b-tensors are empirically chosen, often from uniform sampling of b-tensor parameters[3], typically resulting in on the order of 1000 samples to recover the full DTD[5,6]. To our knowledge, no b-tensor sampling scheme has been proposed for optimally sampling the MD-dMRI signal. We present the first 4D basis for representing the MD-dMRI signal. This enables us to study the properties of the signal in this basis to give recommendations for sampling the space of axisymmetric b-tensor, while enabling accurate reconstruction of the MD-dMRI signal.

MD-dMRI Signal Basis and b-tensor Sampling Scheme

$$\frac{S}{S_0}(\mathbf{B}) = \int P(\mathbf{D})\exp(-\mathbf{B}:\mathbf{D})d\mathbf{D} = \langle\exp(-\mathbf{B}:\mathbf{D})\rangle,$$

is the diffusion signal acquired with b-tensor encoding, where $P(\mathbf{D})$ is the DTD, $\mathbf{D}, \mathbf{B}$ are second order symmetric positive-definite diffusion and b-tensors respectively, and $\mathbf{B}:\mathbf{D} = \sum_i \sum_j b_{ij}D_{ij}$. For a discrete set of diffusion tensor populations,

$$\frac{S}{S_0}(\mathbf{B}) = \sum_{d=1}^{N_D} w_d\exp(-\mathbf{B}:\mathbf{D}_d),$$

where w_d is the proportion of tensor population $\mathbf{D}_d$ and N_D is the number of populations. The axisymmetric diffusion tensor can be parameterised as[5,6],

$$\mathbf{D} = \mathbf{R}(\theta,\phi)D_{iso}\left(\begin{pmatrix}1&0&0\\0&1&0\\0&0&1\end{pmatrix} + D_\Delta\begin{pmatrix}-1&0&0\\0&-1&0\\0&0&2\end{pmatrix}\right)\mathbf{R}(\theta,\phi)^T,$$

where $\mathbf{R}$ is a rotation operator. The b-tensor can be parametrised in terms of (b_s, b_l, Θ, Φ)[2,6],

$$\mathbf{B} = \mathbf{R}(\Theta,\Phi)\left(\frac{b_s}{3}\begin{pmatrix}1&0&0\\0&1&0\\0&0&1\end{pmatrix} + b_l\begin{pmatrix}0&0&0\\0&0&0\\0&0&1\end{pmatrix}\right)\mathbf{R}(\Theta,\Phi)^T.$$

Expanding $\frac{S}{S_0}(\mathbf{B})$, using the above parameterisation, gives a separable expression in b_s, and the other three parameters, b_l, Θ, Φ[2]:

$$\frac{S}{S_0}(\mathbf{B}) = \sum_{d=1}^{N_D} w_d\exp(-b_s(D_{iso})_d)\exp(-b_l(D_{iso})_d)\exp(-2b_l(D_{iso})_d(D_\Delta)_d P_2(\cos\beta_d)),$$

$\cos\beta_d = \cos\Theta\cos\theta_d + \sin\Theta\sin\theta_d\cos(\Phi - \phi_d)$. This enables $\frac{S}{S_0}(\mathbf{B})$ to be expanded in a separable and orthogonal 4D basis which is the product of a 1D basis for b_s dimension and a 3D basis for b_l, Θ and Φ dimensions. As $\frac{S}{S_0}(\mathbf{B})$ is a function of negative exponential of b_s, we use an exponential modulated with a Laguerre polynomial, which together form an orthogonal basis over b_s dimension[7]. Similarly, we use the spherical Laguerre basis[8], a 3D orthogonal basis with an exponential weighting function in the radial direction, for b_l, Θ, Φ dimensions, leading to expansion:

$$\frac{S}{S_0}(b_s, b_l, \Theta, \Phi) = \sum_{p=0}^{P}\sum_{n=0}^{N}\sum_{\ell=0}^{L}\sum_{m=-\ell}^{\ell} c_{pn\ell m}Z_p(b_s)B_{n\ell m}(b_l, \Theta, \Phi)$$

where $B_{n\ell m}(b_l, \Theta, \Phi) = X_n(b_l)Y_\ell^m(\Theta,\Phi)$ is the spherical Laguerre basis, with $X_n(b_l) = \sqrt{\frac{n!}{\zeta_l^3(n+2)!}}\exp(\frac{-b_l}{2\zeta_l})L_n^2(\frac{b_l}{\zeta_l})$, and $Z_p(b_s) = \frac{1}{\sqrt{\zeta_s}}\exp(\frac{-b_s}{2\zeta_s})L_p(\frac{b_s}{\zeta_s})$. $Y_\ell^m(\Theta,\Phi)$ are spherical harmonics of maximum degree L, ζ_l, ζ_s are scale factors and N, P are maximum orders for b_l and b_s bases respectively. Coefficients $c_{pn\ell m}$ are defined by inner product $c_{pn\ell m} = \langle\frac{S}{S_0}(b_s, b_l, \Theta, \Phi), Z_p(b_s)B_{n\ell m}(b_l, \Theta, \Phi)\rangle$. Due to the separability of this basis, we can design a separable transform,

$$c_{pn\ell m} = \sum_{j=0}^{J} w_j Z_p(b_s(j))\sum_{i=0}^{I} w_i X_n(b_l(i))\int_{\Theta=0}^{\pi}\int_{\Phi=0}^{2\pi}\frac{S}{S_0}(b_s(j), b_l(i), \Theta, \Phi)Y_\ell^m(\Theta,\Phi)\sin\Theta d\Theta d\Phi.$$

with Gauss-Laguerre quadrature[9] used to choose the weights w_j, w_i, and sample locations $b_s(j)$, $b_l(i)$ for the b_s and b_l dimensions. We use the scheme[10,11] to place the samples in the angular dimension. For a band-limited signal, this quadrature enables exact reconstruction and efficient sampling with the number of samples equal to number of coefficients.

Methods

The Magic DIAMOND model is used to study maximum orders needed for expansion of the diffusion signal in the proposed basis and to evaluate reconstruction accuracy of the proposed sampling scheme. Magic DIAMOND[12], an extension of the DIAMOND model[13,14] for axisymmetric tensor acquisitions, describes the DTD through a mixture of non-central matrix-variate Gamma distributions, where each diffusion compartment is represented through a single distribution with two shape parameters, that set axial and radial heterogeneity of a compartment, and a scale parameter. Compartments are used to represent diffusion molecules hindered and restricted by fascicles, and free water diffusion. We used a range of diffusivities and distribution parameters representative of those in the human brain.

Results and Discussion

As Magic DIAMOND model is linear, it is sufficient to study each compartment individually; the truncation order of the compartment with the highest truncation order is sufficient to represent all combinations of compartments. Fig.1 shows the spherical harmonic band-limit as a function of b_l. Fig.2 shows the reconstruction error as a function of increasing truncation order for maximum b_l and b_s of $3000 s/mm^2$. It was found that $N = 3$, $P = 2$, $L(i) = [2, 4, 4, 6]$ were sufficient for reconstruction error smaller than $S/S_0 = 0.1$[3] for all compartments, resulting in the sampling scheme (Fig.3) with 192 samples, the same order as several state-of-the-art sampling schemes in q-space[15]. Fig.4 shows the mean reconstruction error evaluated at 1080 uniformly placed measurements for 640 realisations of Magic DIAMOND.

Conclusion

We present the first 4D basis and reconstruction algorithm for representing and reconstructing the axisymmetric b-tensor encoded diffusion signal. We study the properties of the signal to inform how many and which b-tensors should be used, thereby providing sampling recommendations. Although preliminary, the high reconstruction accuracy achieved on Magic DIAMOND model is promising for interpolation of b-tensors encoded measurements to enable algorithms for recovering the DTD to achieve higher accuracy and/or reduce the number of measurements.

Acknowledgements

References

1. D. Topgaard, Chapter 7 NMR methods for studying microscopic diffusion anisotropy, in Diffusion NMR of Confined Systems: Fluid Transport in Porous Solids and Heterogeneous Materials. The Royal Society of Chemistry, 226–259 (2017).

2. D. Topgaard, Multidimensional diffusion MRI, J. Magn. Reson. 275, 98–113 (2017).

3. C.-F. Westin et al., Q-space trajectory imaging for multidimensional diffusion MRI of the human brain, NeuroImage 135, 345–362 (2016).

4. J. P. de Almeida Martins and D. Topgaard, Multidimensional correlation of nuclear relaxation rates and diffusion tensors for model-free investigations of heterogeneous anisotropic porous materials, Scientific Reports 8 (2018).

5. S. Eriksson et al., NMR diffusion-encoding with axial symmetry and variable anisotropy: Distinguishing between prolate and oblate microscopic diffusion tensors with unknown orientation distribution, J Chem Phys. 142, 104201 (2015).

6. J. P. de Almeida Martins and D. Topgaard, Two-dimensional correlation of isotropic and directional diffusion using NMR, Phys. Rev. Lett. 116, 087601 (2016).

7. R. H. Fick et al., Non-parametric graphnet-regularized representation of dMRI in space and time, Med. Image Anal. 43, 37–53 (2018).

8. B. Leistedt and J. D. McEwen, Exact wavelets on the ball, IEEE Trans. Signal Process. 60, 6257–6269 (2012).

9. M. Abramowitz and I. A. Stegun, Handbook of mathematical functions with formulas, graphs, and mathematical tables, ser. National Bureau of Standards Applied Mathematics Series. Dover, New York: U.S. Government Printing Office 55 (1964).

10. A. P. Bates et al., An optimal dimensionality sampling scheme on the sphere with accurate and efficient spherical harmonic transform for diffusion MRI, IEEE Signal Process. Lett. 23, 15–19 (2016).

11. A. P. Bates et al., An optimal dimensionality multi-shell sampling scheme with accurate and efficient transforms for diffusion MRI, in Proc. IEEE Int. Symp. Biomed. Imaging, ISBI, Melbourne, Australia, 770–773 (2017).

12. A. Reymbaut and et al., The "magic DIAMOND" method: probing brain microstructure by combining b-tensor encoding and advanced diffusion compartment imaging, in Proc. Int. Soc. Magn. Reson. Med, Paris, France (2018).

13. B. Scherrer et al., Characterizing brain tissue by assessment of the distribution of anisotropic microstructural environments in diffusion-compartment imaging (DIAMOND), Magn. Reson. Med. 76, 963–977 (2015).

14. B. Scherrer and et al., Decoupling axial and radial tissue heterogeneity in diffusion compartment imaging, in Springer International Publishing, Cham, 440–452 (2017).

15. S. N. Sotiropoulos et al., Advances in diffusion MRI acquisition and processing in the Human Connectome Project, NeuroImage 80, 125–143 (2013).
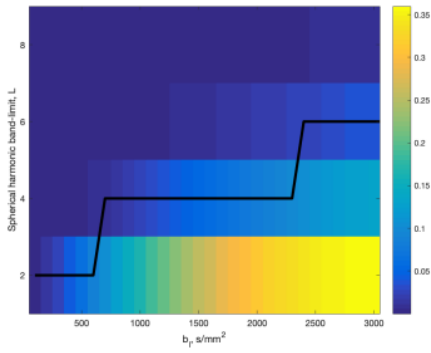
Figures

Fig.1: Maximum absolute reconstruction difference between the reconstructed signal and the ground truth as a function of the spherical harmonic band-limit L and b_l value. L required to accurately represent (maximum absolute reconstruction difference is above $\frac{S}{S_0} = 0.1$, as required by MD-dMRI Gaussian diffusion assumption[3]) the diffusion signal at different b_l-values is shown by the black line.
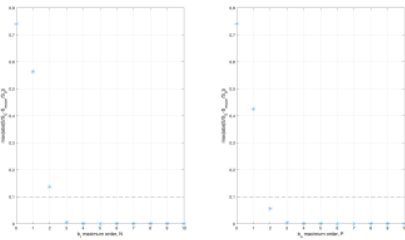

Fig.2: Maximum absolute reconstruction difference between the reconstructed signal and the ground truth as a function of the b_l truncation order N (left) and the b_s truncation order P (right). The truncation order should be high enough so that the reconstruction error is smaller than $\frac{S}{S_0} = 0.1$ (shown by the black line).
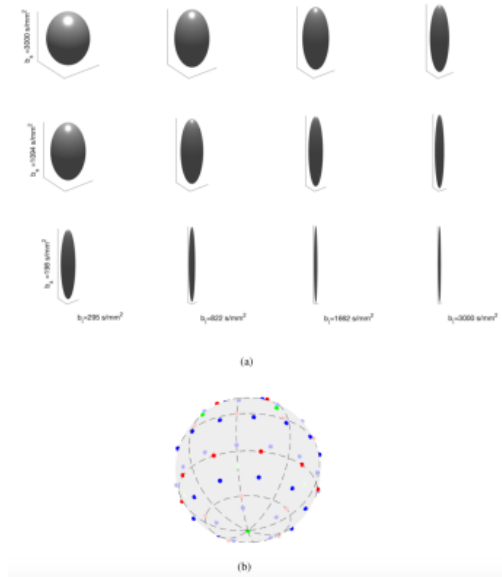

Fig.3: Proposed b-tensor sampling scheme: a) the b-tensors shown for a single orientation, and b) the orientations used in the proposed sampling scheme, projected onto a single sphere, samples on the inner most to outer most shell are shown in green, red (two shells with this sampling) and blue for each shell respectively. Locations where antipodal symmetry is used to infer the value of the signal are lighter in colour.
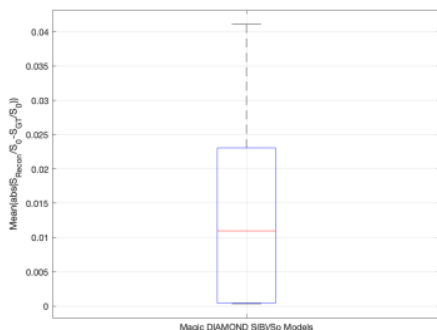
Fig.4: Mean absolute reconstruction error over 1060 uniformly placed samples on a Cartesian grid for 640 realisations of the magic DIAMOND model.